Supporting Information

A new strategy for constructing dispiro-based dopant-free hole-transporting material: spatial configuration of spiro-bifluorene changes from perpendicular to parallel arrangement

Zhongquan Wan,*[a] Jinyu Yang,[a] Jianxing Xia,[a] Hongyu Shu,[a] Xiaojun Yao,[b] Junsheng Luo,[a] and Chunyang Jia*[a]

[a] State Key Laboratory of Electronic Thin Films and Integrated Devices, School of Electronic Science and Engineering, University of Electronic Science and Technology of China, Chengdu 610054, China.

[b] State Key Laboratory of Applied Organic Chemistry, Lanzhou University, Lanzhou 730000, China.

Corresponding authors:

E-mail: zqwan@uestc.edu.cn; cyjia@uestc.edu.cn

1. Experimental procedures

Materials

Chemicals and reagents for material synthesis were purchased from commercial suppliers, such as Aladdin, TCI and so on. The solvents used for material synthesis were dried according to standard procedures. The materials and super dehydrated solvents used for perovskite solar cells fabrication were purchased from Xi'an Polymer Light Technology Corp., Sigma-Aldrich and TCI. Air-sensitive reactions were carried out under nitrogen atmosphere. The perovskite solar cells were fabricated in a glovebox under nitrogen atmosphere.

Perovskite solar cells fabrication

The compact TiO_2 (c-TiO_2) precursor solution was prepared by following steps: 369 μL titanium isopropoxide was added to 2.53 ml ethanol and then stirred. 35 μL 2 M HCl was added to another 2.53 ml ethanol and then stirred. Ethanol with HCl was then added dropwise to the ethanol with titanium isopropoxide with stirring until the solution became clear. The mesoporous TiO_2 (m-TiO_2) solution was prepared by dilute 18NR-T with ethanol in the mass ratio of 1:7. Perovskite precursor was prepared by dissolution 1097.20 mg of PbI_2, 154.14 mg of $PbBr_2$, 380.24 mg of FAI and 43.68 mg of MABr in 2 ml DMF and DMSO (the volume ratio of 4:1) mixing solution. A 103.92 mg of CsI was dissolved in 200 μL DMSO. After fully stirring of the two solution, 68 μL CsI precursor was added to the perovskite precursor solution and then continue stirring. The doped Spiro-OMeTAD solution was prepared by dissolving 72.3 mg of Spiro-OMeTAD in 1 mL of chlorobenzene, to which 28.8 μL of 4-tert-butyl pyridine and 17.5 μL of lithium bis(tri-uromethanesulfonyl)imide (Li-TFSI) solution (520 mg of Li-TFSI in 1 mL of acetonitrile). The dopant-free WH-1 was used with a 20 mg/mL solution in chlorobenzene. Except m-TiO_2, all other solutions must be filtered by using 0.22 μm filter before they can be used.

Device fabrication:[1] FTO substrates were cleaned gradually using detergent solution, alkaline alcohol solution, acetone, deionized water and ethanol. The above steps were operated in

ultrasonic cleaner for 20 minutes respectively. Then, FTO substrates were dried by air flow and treated under UV-ozone for 15 minutes for removing a trace of organic residue. The c-TiO_2 layer was prepared by spin-coating the c-TiO_2 precursor solution on the cleaned FTO substrate and then heated at 150 ℃ for 15 minutes to remove the residual solvent. Then the film was annealed gradually at 500 ℃ for 1 hour and then kept at 500 ℃ for 30 minutes. The m-TiO_2 layer on the FTO/c-TiO_2 substrate was prepared using the 18NR-T dilute solution by using spin-coated method, following with 125 ℃ heating for 10 minutes. The annealing process of m-TiO_2 is the same as that of c-TiO_2. Before preparing the perovskite layer, m-TiO_2 layer was treated with UV-ozone to remove organic residue and improve surface wettability. The perovskite film was deposited on the treated FTO/c-TiO_2/m-TiO_2 substrates by spin-coating filtered perovskite precursor at the speed of 1300 rpm for 10 seconds and 5000 rpm for 45 seconds. During the process of spin-coating, 200 μL chlorobenzene was dropped at the center of the substrates at the last 18 seconds, and then followed by 110 ℃ heating for 60 minutes to complete the phase transition process. Then, the HTM solution was deposited onto the perovskite layer by spin-coating at 3000 rpm for 30 s. Finally, the Au electrode was deposited on the surface of hole-transporting layer by thermal evaporation.

Characterization

^{1}H NMR spectra were recorded on a Bruker AM 400 spectrometer with the chemical shifts against TMS, operating at 400 MHz. High resolution mass spectrometry (HRMS) results were obtained with a Waters LCT Premier XE spectrometer.

Ultraviolet-visible (UV-Vis) absorption spectra were measured on a model Mapada UV-6100 spectrophotometer at room temperature in CH_2Cl_2 with a conventional 1 cm quartz cell. Emission spectra were recorded on a Fluoromax-4 spectrofluorometer (HORIBA JobinYvon). Cyclic voltammetry (CV) experiments were performed on a CHI 660E electrochemical workstation (Shanghai Chenhua) at a scan rate of 50 mV s^{-1} in CH_2Cl_2 (5×10^{-4} M) containing 0.1 M tetrabutylammonium hexafluorophosphate (*n*-Bu_4NPF_6) as the supporting electrolyte,

with a three electrode configuration, consisting of a Ag/AgCl (saturated KCl) reference electrode, a Pt wire counter electrode and a Pt disk working electrode.

Thermo gravimetric analysis (TGA) was carried out with a TA Instruments TGA-Q50 at a heating rate of 10 °C min^{-1} from room temperature to 800 °C under nitrogen atmosphere. Difference scanning calorimetry (DSC) analysis was performed using TA Instruments modulated DSC-Q100 at a heating rate of 10 °C min^{-1} under nitrogen atmosphere.

Steady-state photoluminescence (PL) spectra were measured by HITACHI (model F-4600) spectrophotometer with the excitation wavelength of 460 nm. Time-resolved photoluminescence (TRPL) spectra was measured by using a time-correlated single photon counting (TCSPC) technique at room temperature. The instrument for TRPL measurement was FluoroLog-3 Modular spectrofluorometer (HORIBA Jobin Yvon) with the emission wavelength of 760 nm.

Scanning electron microscopy (SEM) images were observed by SEM (JEOL JSM-7600F). Atomic force microscopy (AFM) images were observed by Atomic force microscopy (Bruker Dimension Icon). Water contact angles of HTM films were performed by drop shape analyzer (Krüss DSA100).

The optimized structures and frontier orbitals of HTMs were carried out by using the density functional theory (DFT) and B3LYP/6-31G* program with the Gaussian 09.[2]

The hole-transporting mobility was determined from hole-only devices with structure of ITO/PEDOT:PSS/HTM layer/MoO_3/Al using the space charge limited current (SCLC) method. The *J-V* curves of the PSCs were measured using an electrochemical workstation (CHI 660E, Shanghai Chenhua) under AM 1.5G simulated solar light and ambient atmosphere (100 mW cm^{-2}) (CHF-XM-500W, Trusttech Co. Ltd., China) (scan rate = 50 mV s^{-1}). The incident light intensity was calibrated with a standard Si solar cell. The active area of the PSC device was defined by the cross area of top and bottom electrodes and a home-made black metal mask of 0.09 cm^{-2}. The incident photon-to-electron conversion efficiency (IPCE) spectra were

performed by using QTest Station 2000 IPCE Measurement System (CROWNTECH, USA). The 60 days stability test of unpackaged PSCs stored under dark ambient conditions with a humidity of 50-70% at room temperature (about 25 ℃) was carried out under ambient atmosphere.

2. Synthetic details

The synthetic route to WH-1 is shown in Scheme S1, which shows a straightforward synthesis process with a simple two-step synthetic procedure from commercially available starting material 2,7-dibromo-9H-fluorene.

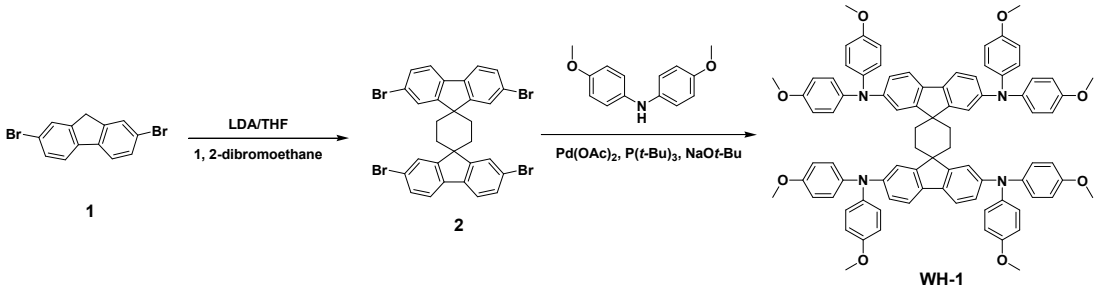

Scheme S1 The synthetic route of WH-1.

Synthesis of Dispiro Core 2.[3] Lithium diisopropylamide (2.75 ml, 5.5 mmol) was added dropwise into a solution of 2,7-dibromo-9H-fluorene (1.62 g, 5 mmol) in THF under nitrogen at room temperature. The solution was stirred at room temperature for 1 hour, and then 0.215 ml 1,2-dibromoethane (2.5 mmol) was added dropwise to the mixture solution. The mixture solution continued to be stirred for 1 hour and poured into water and extracted with ether. The organic extracts were dried over $MgSO_4$ and evaporated. The residue was purified by silica gel column chromatography (hexane) to provide the dispiro core 2 as a white solid. (1.42 g, 82% yield). MS-ESI (m/z): calcd. for $[M]^+$ calcd for $C_{30}H_{20}Br_4$ 695.8, found: 695.8.

Synthesis of WH-1.[4] The synthesis of compound WH-1 was obtained by Buchwald-Hartwig reaction. 4,4'-dimethoxydiphenylamine (1.52 g, 6.62 mmol), dispiro core 2 (1.07 g, 1.54 mmol) and NaOtBu (0.74 g, 7.7 mmol) were added to 30 ml dry toluene. The system was purged with nitrogen three times. Then $P(t\text{-}Bu)_3$ (0.03 g, 0.124 mmol) and $Pd(OAc)_2$ (0.03 g, 0.124 mmol)

were placed in the mixture solution, and the reaction was refluxed overnight. Organic phase separation by ethyl acetate and combined organic phase was dried with $MgSO_4$. The organic phase was concentrated, and the residue was purified with silica gel column chromatography (hexane/ethyl acetate) to afford 1.49 g (yield 75%) of WH-1. ^{1}H NMR (400 MHz, DMSO-d_6, 298 K), δ (ppm): 7.57 (d, J = 8Hz, 4H), 6.96 (d, J = 8 Hz, 4H), 6.88 (d, J = 12Hz, 4H), 6.77~6.74 (dd, $J1$=4 Hz, $J2$= 4 Hz, 16H), 6.59 (d, J = 4Hz, 16H), 3.73 (s, 24H), 1.99 (s, 8H). HRMS-ESI (m/z): $[M+H]^+$ calcd for $C_{86}H_{76}N_4O_8$ 1293.5663, found: 1293.5741.

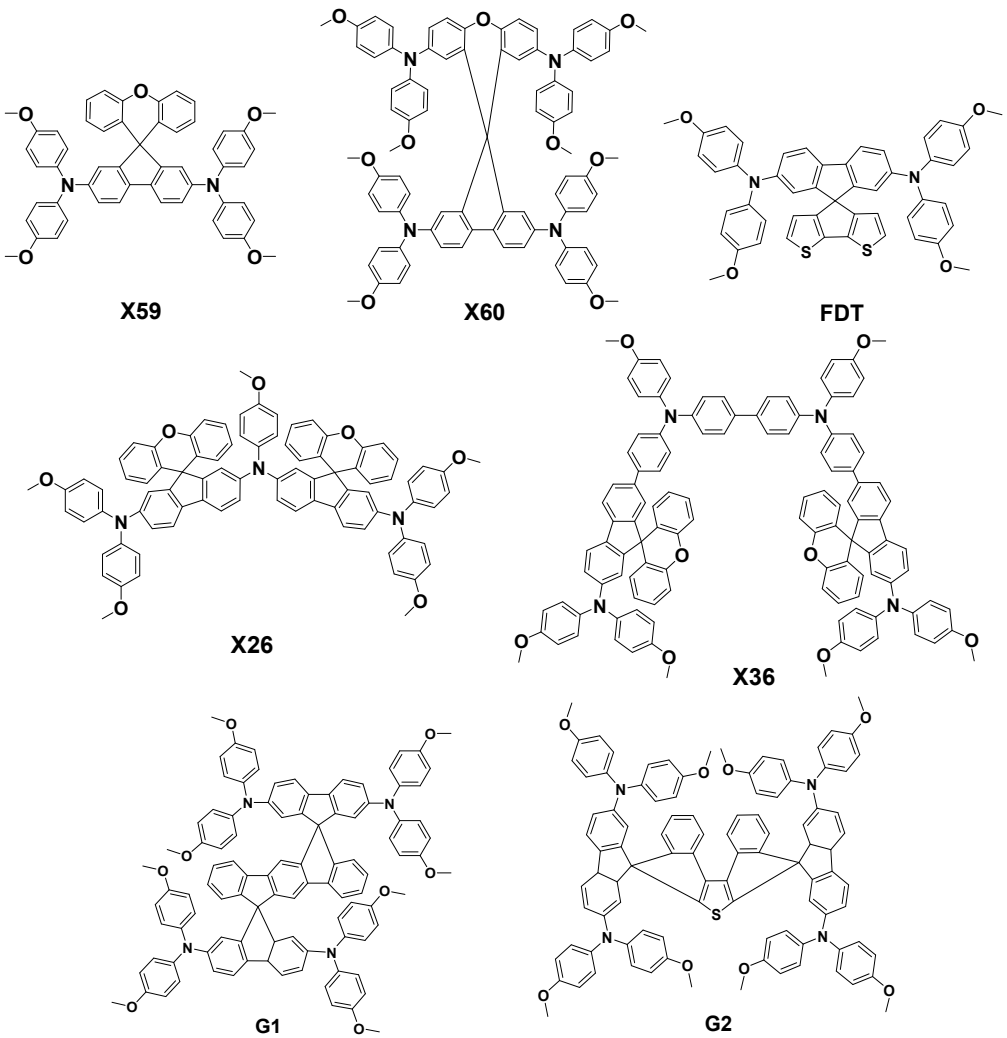

Fig. S1 The chemical structures of the hole-transporting materials mentioned in the introduction.

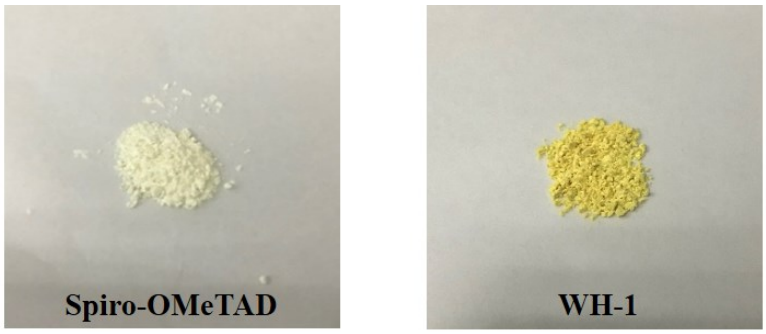

Fig. S2 Optical photos of hole-transporting materials.

Table S1 Materials, quantities and cost for the synthesis of WH-1.

Chemical	Weight Reagent (g/g)	Weight Solvent (g/g)	Weight Workup (g/g)	Price of Chemical ($/kg)	Cost of chemical ($/g Product)	Total cost ($/g)
2,7-dibromo-9H-fluorene	1.14			308.43	0.35	
Lithium diisopropylamide	1.68			44.62	0.07	
1,2-Dibromoethane	0.33			24.98	0.01	
THF		17.74		9.94	0.18	
$MgSO_4$			10	8.77	0.09	
Silica gel			265	7.54	2.00	
Hexane			528	6.79	3.58	
Dispiro Core 2	3.15	17.74	803			6.28
Dispiro Core 2	0.72			6280	4.51	
4,4'-dimethoxydiphenylamine	1.02			11657	11.89	
NaOtBu	0.50			49.16	0.02	
$P(t\text{-}Bu)_3$	0.02			2218.49	0.05	
$Pd(OAc)_2$	0.02			47900.21	0.96	
toluene		25.98		6.66	0.17	
ethyl acetate			451	3.63	1.64	
$MgSO_4$			10	8.77	0.09	
Silica gel			265	7.54	2.00	
Hexane			330	6.79	2.24	
WH-1	2.28	25.98	1056			23.57

3. DFT calculations

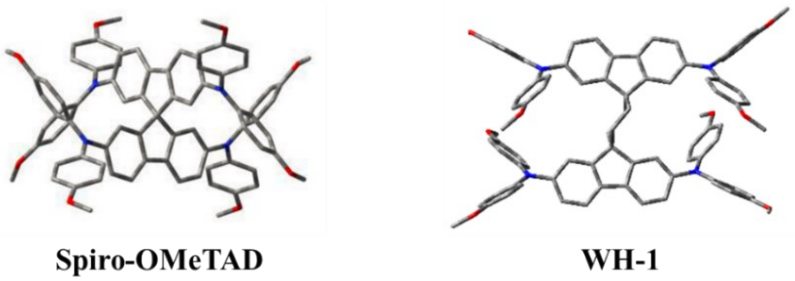

Fig. S3 The side view derived of the optimized structures from DFT calculations.

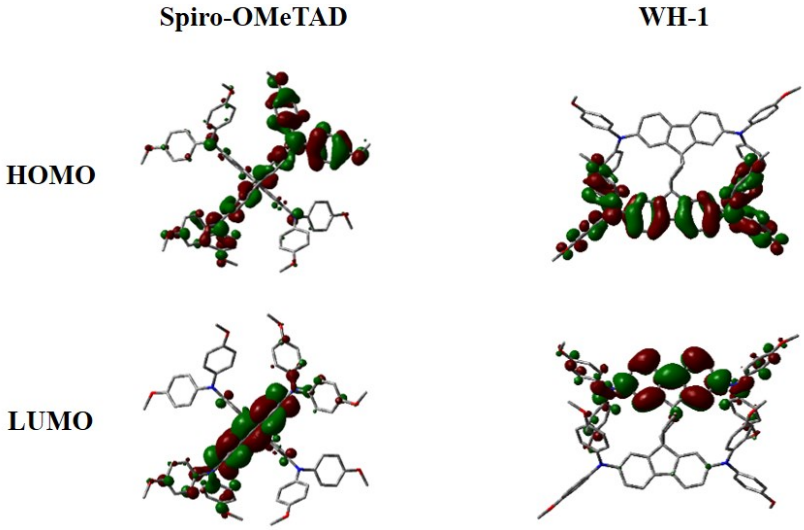

Fig. S4 HOMO and LUMO orbitals obtained from density functional theory/B3LYP calculations using the 6-31G* basis set.

4. TGA thermograms

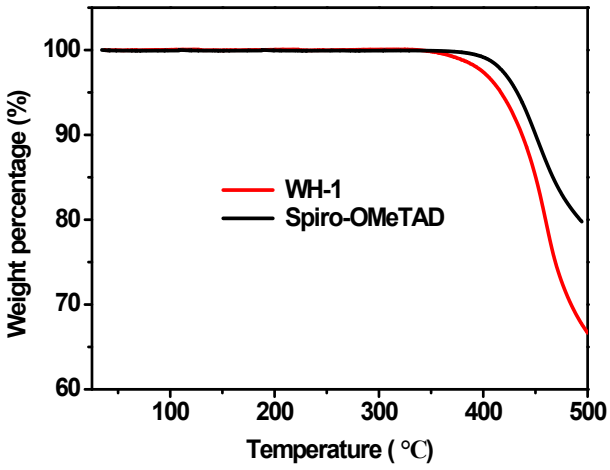

Fig. S5 TGA thermograms at a scan rate of 10 °C min^{-1} under N_2 atmosphere.

5. Device performances

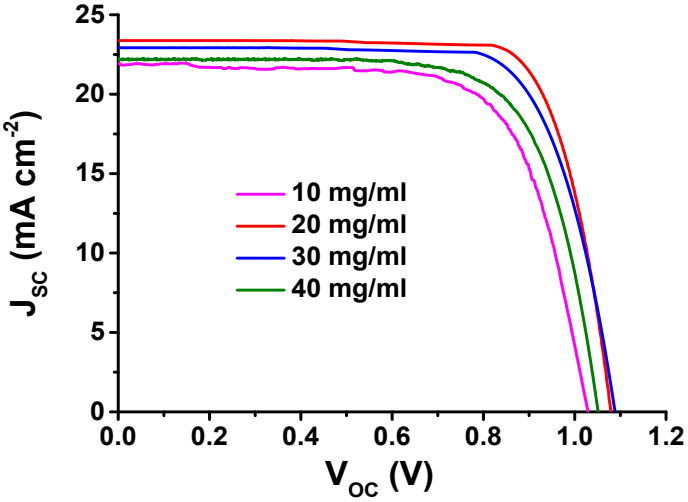

Fig. S6 *J–V* curves with reverse scanning of PSCs based on WH-1 with different concentrations.

Table S2 Photovoltaic parameters of PSCs based on WH-1 with different concentrations.

Concentrations	J_{sc} [mA cm^{-2}]	V_{oc} [V]	*FF* [%]	PCE [%]
10 mg/ml	21.94	1.03	69.90	15.78
20 mg/ml	23.37	1.08	77.54	19.57
30 mg/ml	22.93	1.09	73.76	18.40
40 mg/ml	22.19	1.05	72.18	16.82

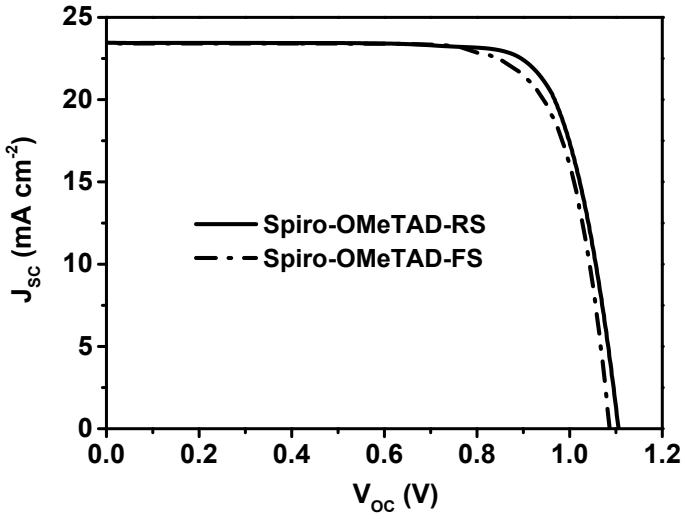

Fig. S7 *J-V* curves of PSCs at backward and forward scan with doped Spiro-OMeTAD.

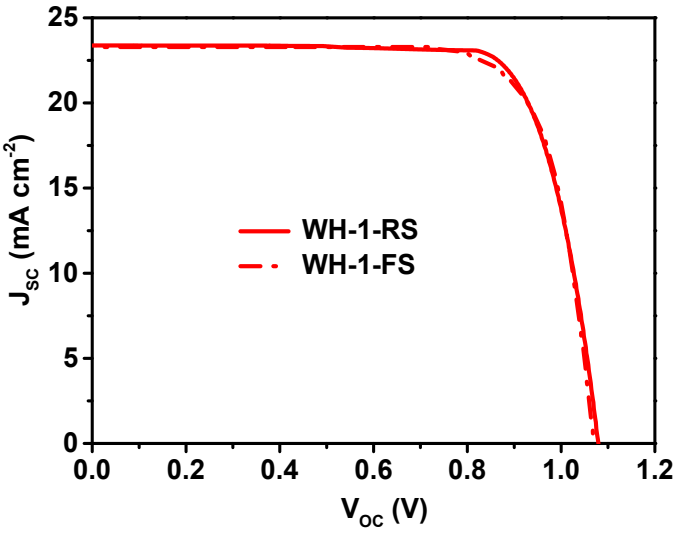

Fig. S8 *J-V* curves of PSCs at backward and forward scan with dopant-free WH-1.

Table S3 Photovoltaic parameters derived from *J–V* measurements of the champion PSCs under reverse and forward scan.[a]

HTM	Scan direction	J_{sc} [mA cm^{-2}]	V_{oc} [V]	*FF* [%]	PCE [%]	H-index[d] [%]
Spiro-OMeTAD	RS[b]	23.46	1.11	77.94	20.29	+4.63
	FS[c]	23.41	1.09	75.85	19.35	
WH-1	RS	23.37	1.08	77.54	19.57	+2.50
	FS	23.29	1.07	76.58	19.08	

[a] Measured under AM 1.5G (100 mW cm^{-2}); [b] RS: reverse scan; [c] FS: forward scan; [d] H-index =($PCE_{reverse}$ - $PCE_{forward}$)/$PCE_{reverse}$.

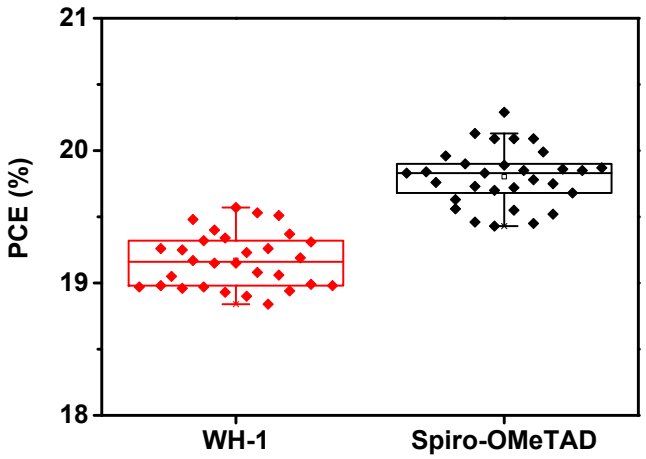

Fig. S9 Statistical PCEs of 30 devices based on different HTMs.

References

1. H. Shu, J. Xia, H. Yang, J. Luo, Z. Wan, H. A. Malik, F. Han, X. Yao and C. Jia, *ACS Sustainable Chem. Eng*., 2020, **8**, 10859-10869.

2. Gaussian 09, Revision D.01, M. J. Frisch, G. W. Trucks, H. B. Schlegel, G. E. Scuseria, M. A. Robb, J. R. Cheeseman, G. Scalmani, V. Barone, B. Mennucci, G. A. Petersson, H. Nakatsuji, M. Caricato, X. Li, H. P. Hratchian, A. F. Izmaylov, J. Bloino, G. Zheng, J. L. Sonnenberg, M. Hada, M. Ehara, K. Toyota, R. Fukuda, J. Hasegawa, M. Ishida, T. Nakajima, Y. Honda, O. Kitao, H. Nakai, T. Vreven, J. A. Montgomery, Jr., J. E. Peralta, F. Ogliaro, M. Bearpark, J. J. Heyd, E. Brothers, K. N. Kudin, V. N. Staroverov, T. Keith, R. Kobayashi, J. Normand, K. Raghavachari, A. Rendell, J. C. Burant, S. S. Iyengar, J. Tomasi, M. Cossi, N. Rega, J. M. Millam, M. Klene, J. E. Knox, J. B. Cross, V. Bakken, C. Adamo, J. Jaramillo, R. Gomperts, R. E. Stratmann, O. Yazyev, A. J. Austin, R. Cammi, C. Pomelli, J. W. Ochterski, R. L. Martin, K. Morokuma, V. G. Zakrzewski, G. A. Voth, P. Salvador, J. J. Dannenberg, S. Dapprich, A. D. Daniels, O. Farkas, J. B. Foresman, J. V. Ortiz, J. Cioslowski, and D. J. Fox, Gaussian, Inc., Wallingford CT, 2013.

3. D. J. Park, Y. Y. Noh, C. M. Chun, J. Kim and D. Y. Kim, *Mol. Cryst. Liq. Cryst*., 2002, **377**, 73-76.

4. B. Xu, D. Bi, Y. Hua, P. Liu, M. Cheng, M. Grätzel, L. Kloo, A. Hagfeldt and L. Sun, *Energy Environ. Sci*., 2016, **9**, 873-877.